AMERICAN JOURNAL of PHYSICS

Volume 74, No. 10, October 2006

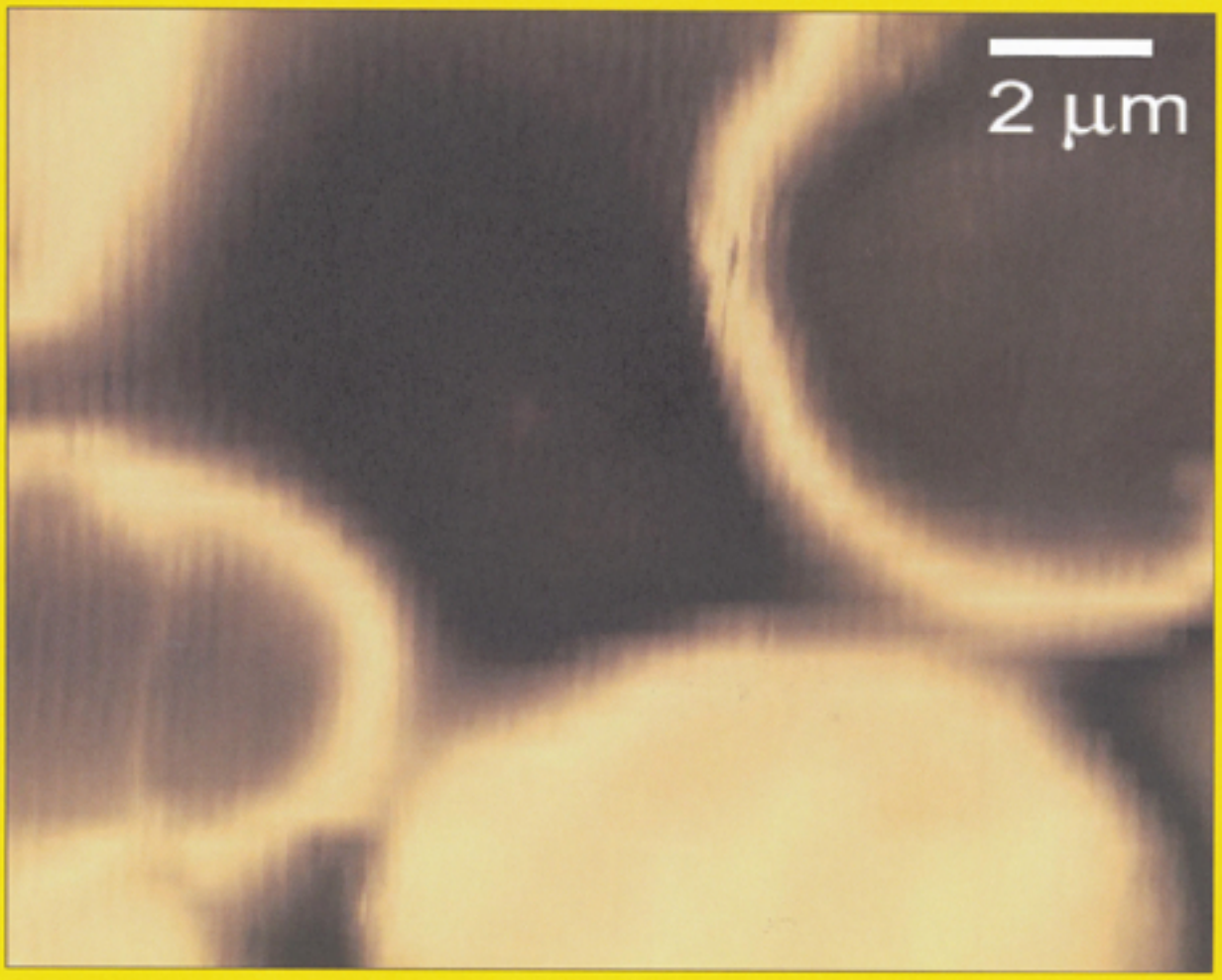

A PUBLICATION OF THE AMERICAN ASSOCIATION OF PHYSICS TEACHERS

Available online—visit http://aapt.org/ajp

AMERICAN JOURNAL of PHYSICS

CODEN: AJPIAS
ISSN: 0002-9505

Volume 74, No. 10
October 2006

Cover figure: A sample image taken with the AFM of human red blood cells, imaged in air after they were dried on a glass substrate. The image is 15 μm square, and consists of 32 lines of data with 250 data points acquired per line. The image was linearly interpolated and up-sampled to 400×400 pixels. The blood cells in the image belonged to MIT's Professor Linda Griffith. See the article on page 873.

(Continued)

Measuring Boltzmann's constant with a low-cost atomic force microscope: An undergraduate experiment

M. Shusteff, T. P. Burg, and S. R. Manalis[a)]
Biological Engineering Division, Massachusetts Institute of Technology, Cambridge, Massachusetts 02139

(Received 25 January 2006; accepted 14 July 2006)

We discuss a low-cost atomic force microscope that we have designed and built for use in an undergraduate teaching laboratory. This microscope gives students hands-on access to nano-Newton force measurements and subangstrom position measurements. The apparatus relies mainly on off-the-shelf components and utilizes an interferometric position sensor known as the interdigitated (ID) cantilever to obtain high resolution. The mechanical properties of the ID readout enable a robust and open design that makes it possible for students to directly control it. Its pedagogical advantage is that students interact with a complete instrument system and learn measurement principles in context. One undergraduate experiment enabled by this apparatus is a measurement of Boltzmann's constant, which is done by recording the thermal noise power spectrum of a microfabricated cantilever beam. In addition to gaining an appreciation of the lower limits of position and force measurements, students learn to apply numerous concepts such as digital sampling, Fourier-domain analysis, noise sources, and error propagation. © *2006 American Association of Physics Teachers.*

[DOI: 10.1119/1.2335475]

I. INTRODUCTION

New approaches to quantitative measurement are important for advancing many areas in science and engineering. These measurements require an increasingly diverse range of instrumentation and a multidisciplinary background to be carried out successfully. It is crucial that students understand not only the physical principles underlying a particular phenomenon, but also the behavior and limitations of the measurement system used to observe it. In many cases students with interests at the interface of biology, physics, and engineering receive little exposure to measurement and instrumentation. As a result, they may perceive state of the art measurement systems as black boxes,[1] with little understanding of how a measurement is made, why it is done in a particular way, and what affects its outcome.

We see a tremendous benefit in teaching an undergraduate laboratory involving a complete measurement system on which a student can "turn all the knobs," that is, learn about the interaction of all its parts, from transducer to signal generation and amplification to data sampling, recording, and analysis. To this end, we have designed and built an inexpensive atomic force microscope (AFM) system that enables this type of hands-on learning, while retaining the essential functionality of a fully featured commercial AFM.

The apparatus is assembled largely from off-the-shelf components at less than a tenth of the cost of a research-grade AFM. Commercial AFM systems are less practical to use as teaching tools primarily due to their expense and minimal access to their inner workings. Having more than one setup is unlikely, and when more than two or three students must cluster around a single instrument, only limited learning is possible, especially if students do not operate the tool themselves.

Our AFM is deliberately built for transparency and accessibility. At every stage in the signal path, students have the opportunity to understand the underlying physical principles and interact with the system parameters. Some of the accessible topics include diffraction and Fourier optics underlying the interferometric detection, basic electronic instrumentation, sampling, and discrete-time signal processing and Fourier analysis of recorded data. It is also possible to configure the instrument for students who are only familiar with a few of these areas, so that a subset of these topics may be taught.

Using this AFM, students gain direct and hands-on experience with a complete measurement system that is relevant to many areas of modern physical, materials, and biological research. Of several experiments enabled by the apparatus, we describe here one in which Boltzmann's constant can be measured from the thermomechanical noise of a freely vibrating microcantilever probe. In addition to the value of learning about noise in the context of measurement, the relation between temperature and energy yields insight into the fundamental limits of nanoscale position and force measurements. Furthermore, thermally driven vibrations are a major consideration in state-of-the-art systems and are often the limiting factor for such measurements. During the experiment, students learn the practical relevance of various concepts encountered in the classroom, such as frequency-domain signal analysis, sampling, bandwidth, and noise considerations.

We have used these AFMs to offer three weeks of experiments as part of an undergraduate laboratory course on measurement and instrumentation. Our lab accommodates ten students at a time, who work in pairs on five AFM setups. These third- and fourth-year students came from a variety of backgrounds, including mechanical and chemical engineering and biology, and all were able to acquire the theoretical foundations and the experimental skills needed for the lab through a combination of classroom instruction and hands-on sessions with the instruments.

II. ENABLING TECHNOLOGY: ID SENSOR

At the heart of an atomic force microscope is a microfabricated probe with a sharp tip, which interacts with the sample of interest.[2] Forces and distances are measured by monitoring the bending of a microcantilever beam, on which the tip is mounted.

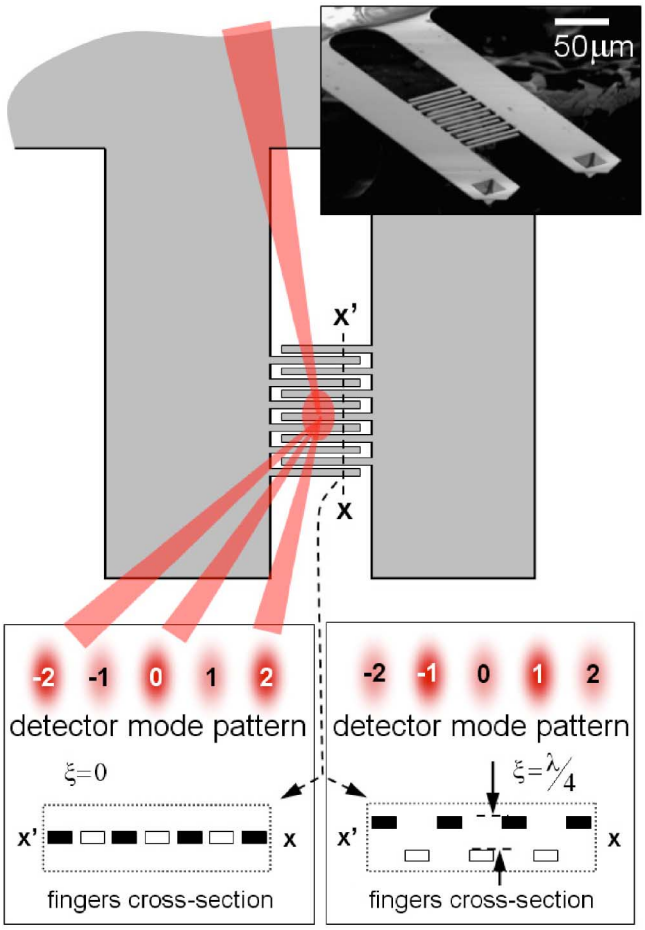

Fig. 1. A schematic that illustrates the operational principle of the ID sensor, with the detection laser shown incident from the top of the figure. When both finger sets are aligned (left box), the even-numbered diffraction orders are brightest and the odd ones are the darkest. When one of the finger sets displaces out of plane by a distance equal to one quarter of the laser wavelength, the situation reverses (right box). This repeats every $\lambda/4$ in either direction. The inset shows the geometry of a pair of cantilevers used for the experiment described in Sec. III.

To measure cantilever bending we use an interferometric approach known as the interdigitated (ID) cantilever.[3] This approach differs from the technique used in commercial AFMs in that, rather than detecting the position of a laser reflecting off the cantilever,[4] we observe the intensity of a diffracted beam. This method is sensitive enough to detect subangstrom cantilever motions, yet it is relatively insensitive to vibrations and mechanical noise in the optical path and has minimal alignment requirements. This system is therefore robust and relatively easy to use, but retains sufficient precision to make interesting measurements.

The schematic in Fig. 1 summarizes the detection mechanism. A laser beam is incident on the ID grating and reflects as several diffraction orders, referred to as "modes," whose intensity depends on the relative out-of-plane displacement between finger sets. One of the finger sets is attached to the probe cantilever, and the other to an identical cantilever or a fixed structure, depending on the desired measurement. By observing the intensity of the diffracted modes, we measure the displacement of one set of fingers relative to the other, which is an inherently referenced measurement.

A central characteristic of the ID system is the nonlinear

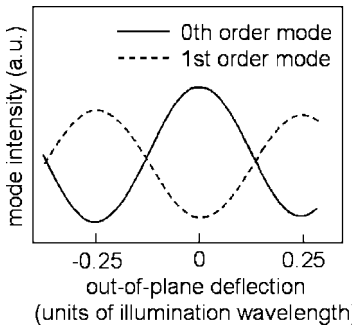

Fig. 2. The nonlinear intensities of the zeroth- and first-order modes plotted as a function of out of plane finger displacement. See Refs. 5 and 6 for details.

dependence of the mode intensities on cantilever deflection: The intensity I of odd-order modes as a function of relative out-of-plane finger displacement ξ has the form

$$I \propto \sin^2\left(\frac{2\pi}{\lambda}\xi\right), \tag{1}$$

where λ is the wavelength of the illumination laser.[5,6] (For even modes, the sine is replaced by a cosine.) The plot in Fig. 2 is a sketch of the intensities of two adjacent modes as a function of the displacement, based on modeling the diffraction of the ID fingers.[5] The analytical details and the results of the simulation are available in Refs. 5 and 6. The key result is that the brightness of a single mode goes from maximum to minimum as the fingers displace a distance of $\lambda/4$. Therefore, an advantage of this sensor is that it can be calibrated in a straightforward way based on the wavelength of light. Calibration procedures are discussed in Sec. III B.

III. EXPERIMENT

Undergraduates are able to perform a number of experiments with this AFM system, several examples of which are given in Sec. VI. We discuss here one experiment that is particularly relevant in statistical mechanics: a measurement of Boltzmann's constant k_B. The procedure takes only a few hours and is rich with learning opportunities.

The approach we take stems from modeling the thermally induced vibrations of the cantilever as a one-dimensional harmonic oscillator. The oscillator's instantaneous total energy is the sum of its kinetic and potential energies

$$E = \frac{1}{2}m\left(\frac{dz}{dt}\right)^2 + \frac{1}{2}kz^2, \tag{2}$$

where m is the effective oscillator mass, k is its spring constant, and z denotes its displacement from equilibrium.

By the equipartition theorem, the average potential energy imparted by the thermal fluctuations is related to the ambient temperature by

$$\tfrac{1}{2}k_BT = \tfrac{1}{2}k\langle z^2\rangle, \tag{3}$$

where $\langle z^2\rangle$ is the mean-square displacement, and T is the absolute temperature.

The approach takes advantage of the sensitive position detector to measure the vibrations of the microfabricated beam, which is driven only by the ambient thermal energy.

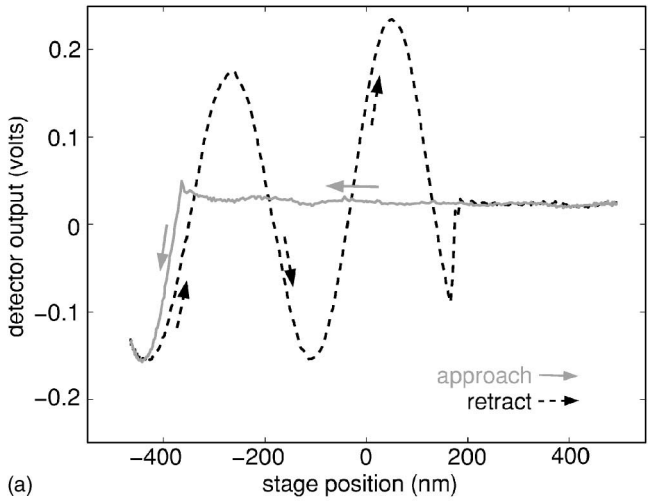

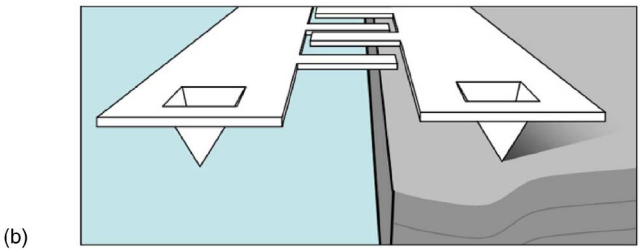

Fig. 3. (a) A typical force curve measured with the ID detector (more negative x-axis values correspond to a higher stage position). Approach and retraction are shown by different line types, and arrows indicate the direction of motion. Several non-idealities of a measured force curve, as compared to the theoretical ID output shown in Fig. 2, are apparent: the variation in amplitude of the $\sin^2$ curve is due to angle mismatch that arises as the cantilever bends; hysteresis between the approach and retraction portions of the curve is due to forces between the tip and the sample. The difference in location between the contact and release points is discussed in the text. (b) A sketch of the method used to bend one of the cantilevers against the edge of a sample.

Using this vibration data and the beam's stiffness k, Eq. (3) can then be solved for Boltzmann's constant k_B.

The experiment consists of three main steps: First, the AFM is run in force-curve mode to calibrate the output. Second, the tip is held away from any sample surfaces, and the intensity signal of a single diffraction order is recorded at high gain as a function of time. Third, the power spectrum of this signal is calculated and analyzed to extract the relevant model parameters.

A. Measuring force-versus-distance curves

To obtain quantitative measurements, the output curve of the ID detector is calibrated by operating the AFM in a "force curve" regime, in which the sample stage is actuated strictly up and down, with the probe tip in close proximity. As the sample oscillates, the tip alternately makes contact, bending the cantilever, and releases from the surface.

In this mode, sensor output is plotted as a function of stage position (and therefore cantilever deflection, when in contact). This output curve is readily observed on an oscilloscope in the X-Y mode, with the detector signal on the vertical axis, and the stage-actuation signal on the horizontal. A typical force curve is shown in Fig. 3(a).

The oscillating section of the curve corresponds to the bending of the cantilever, and the flat section corresponds to the detector output remaining unchanged while the cantilever is off the surface. A noticeable hysteresis is seen between the upward and downward movement of the stage, the degree of which can vary depending on the tip-sample interaction. In particular, the difference in stage height between the contact and release points can be used to measure the adhesion force between the tip and the sample.

B. Biasing and calibration

Because the ID sensor is inherently nonlinear, the measurement sensitivity depends critically on the operating point or bias. For maximum sensitivity the ID output should be biased to the region of greatest slope along the $\sin^2$ curve, which is midway between the maximum and minimum. Due to residual strain in the silicon nitride from which the cantilevers are fabricated, the relative planar alignment of the two finger sets varies slightly over the area of the ID grating. This variation is most pronounced in the lateral direction between the two cantilevers and is typically a few hundred nanometers. Therefore, the bias point of the detector's output can be adjusted along the $\sin^2$ curve by moving the incident laser spot side to side on the diffraction grating.

An alternate approach for biasing involves bending the cantilever until the detector output comes to the desired point. Although this method is impractical if a pair of cantilevers is used for the thermal noise measurement, it is useful when using the ID sensor for AFM imaging.

For small displacements about the chosen bias point, the detector's voltage-to-displacement relation A_{cal} can be expressed as follows:

$$A_{\mathrm{cal}} = \frac{\lambda/4}{V_\lambda} m_{\sin} F_{\mathrm{corr}}. \tag{4}$$

Here V_λ is the x-axis voltage distance from peak to trough on the output curve (corresponding to an out-of-plane distance of $\lambda/4$), and $m_{\sin}$ is the slope of the output curve at the desired bias point (in V_x/V_y). Finally, F_{corr} is a unitless geometric correction factor[7] that relates the tip displacement to measured displacement at the ID grating (the ID fingers deflect less than the end of the cantilever, because they are attached some distance away from the end).

The calibration procedure for thermomechanical noise measurement requires deflecting one of the two matched cantilevers against the edge of a hard substrate, while the other hangs free and undeflected, as shown in Fig. 3(b). The calibration factor and bias point are then determined from the resulting force curve. For this measurement the bias must be set to give maximally sensitive output with the cantilever out of contact. This optimal bias point is set by adjusting the lateral laser position on the grating until the flat portion of the curve joins the oscillating section midway between the maximum and minimum [see Fig. 3(a)].

For students without prior experience in quantitative measurements, understanding these operations is nontrivial and highly instructive. The necessity of proper biasing, coupled with the calibration calculations, are concepts that generalize well to similar biasing and calibration concerns in other measurement systems. Teaching students how the signals observed on instrument displays relate to physical phenomena, and how to extract quantitative data from them is the major goal of an instrumentation and measurement laboratory.

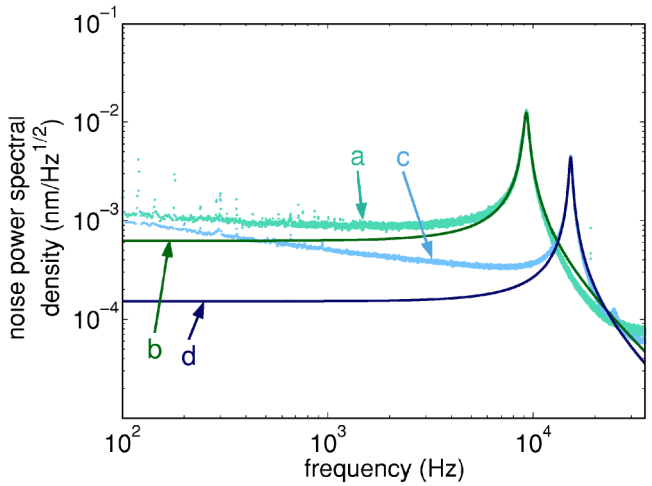

Fig. 4. PSD data (curves "a" and "c") and corresponding fit functions (curves "b" and "d") for 350 and 275 μm long cantilevers, respectively. See the text for a discussion of fitting, and Sec. V for the theoretical background.

C. Spectral data

Once the output is properly adjusted, the movement of the sample for visualizing the force curve is halted, the cantilever is lifted away from the surface, and its thermomechanical noise spectrum is recorded at a high detector gain. The use of two identical cantilevers helps to cancel common-mode effects, such as drifts caused by air currents or temperature fluctuations. It also allows for very clean spectra with virtually no extraneous peaks to complicate the data. The one-sided power spectral density (PSD) of the ID noise signal is calculated using a simple LABVIEW spectral analyzer. The PSD data is divided by a factor of $\sqrt{2}$ to obtain the absolute deflection of a single cantilever from the measured deflection of both beams relative to each other. Typical spectra are shown in Fig. 4, with fitted model second-order transfer functions overlaid on the data.

Fitting is done using MATLAB using the LSQCURVEFIT routine to a function of the following form (see Sec. V for a derivation):

$$S_{zz}(\omega) = \sqrt{\frac{4k_BT}{Qk\omega_0}}\sqrt{\frac{1}{(1-\omega^2/\omega_0^2)^2+\omega^2/Q^2\omega_0^2}}. \tag{5}$$

The parameters ω_0 and Q are the angular resonant frequency and quality factor of the oscillator, respectively, which the fit allows us to extract with good accuracy. Section V describes these and other model parameters in detail and how they are used to calculate k_B.

IV. APPARATUS DETAILS

The AFM consists of several subsystems: The ID cantilever probe, whose position is read by the detection laser, its optics, and readout electronics; the sample positioning stage, piezo-scanner, and driving electronics; and the computer and data acquisition system; complete parts lists, design details, and drawings are available.[8]

A. Interdigitated cantilevers

The ID cantilevers are microfabricated using a well-established silicon nitride process that was originally described by Albrecht *et al.*[9] Using this method, we fabricated approximately 500 devices per 150 mm wafer, with a yield of over 90%, using the facilities at the MIT Microsystems Technology Laboratories. The details of the processing steps and mask layouts are available online.[8]

This process can be implemented at most microfabrication facilities, such as one of the member sites of the NSF-supported National Nanotechnology Infrastructure Network.[10] These university facilities provide microfabrication expertise and infrastructure to research and educational users. At the MIT facility, we estimate that fabricating a batch of 25 wafers (each containing 400 devices) would take about two months and cost approximately $20 000 for materials, machine usage, and labor. Thus, 10 000 devices can be produced at a cost of approximately $2 per device. We anticipate that a group of universities could undertake this production while requiring only a modest initial investment of funds. Because only 10–100 devices are consumed for each semester of the course, the devices from a single process run could support AFMs in teaching labs at these universities for over a decade.

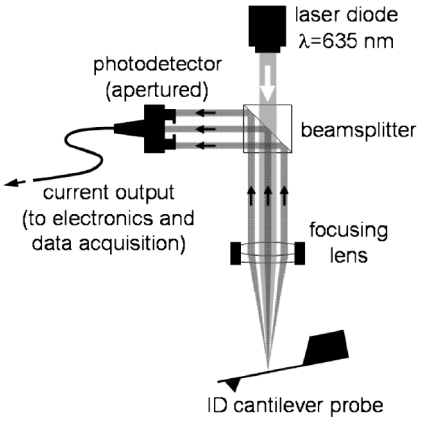

Fig. 5. Schematic of the optical path.

B. Optical and electrical signal paths

The detection optics (ThorLabs) of the AFM are mounted on a single-piece head assembly, laid out as sketched in Fig. 5. The probe's ID fingers are illuminated by a $\lambda = 635$ nm, 5 mW diode laser, operated in constant-power mode. The laser is collimated, then focused onto the diffraction grating, and the diffractive modes are steered by the beamsplitter onto the photodiode detector as they reflect upward.

The photodiode's current output needs minimal processing. For this experiment the output requires conversion to a voltage at a total gain of 10^8 V/A, which is achieved using a 100 kΩ resistor followed by a gain of 10^3 provided by a Tektronix voltage amplifier. The output is observed using an oscilloscope and recorded using a personal computer with data acquisition hardware (National Instruments NI-DAQ).

C. Sample positioning system

The cantilever is held fixed with a machined quartz probe holder (Veeco). The sample is mounted on a three-axis micrometer-driven stage (Newport) for coarse positioning, and supplemented by a piezodisk actuator for fine movements. The disk is divided into quadrants and flexes when

Table I. Approximate cost of major AFM system components.

PC with NI-DAQ system	$3000
Optics and supporting components	1700
Newport three-axis sample positioning stage	1500
New Focus picomotor and joystick	1500
Veeco fluid cell/cantilever holder	1000
Oscilloscope, voltage amp, and instrument chassis	1000
Piezoactuator and associated electronics	200

differential voltages are applied, moving the sample in the x-y plane by means of an offset post. Motion along the z axis (for taking force curves) is achieved by applying a common voltage to all four piezo quadrants. Therefore, the piezo is capable of all three axes of motion needed for scanning and force measurements.

Only moderate voltages (±40 V) are needed to obtain several microns of lateral and vertical displacement. Actuation is accomplished by outputting appropriate voltage waveforms from the data input-output system using MATLAB, and amplifying them 4× using a simple op-amp circuit (Acopian, Analog Devices).

Finally, the calibration procedure requires fine position adjustment along the z axis with a greater range of travel than the piezodisk can achieve. Such positioning is accomplished by means of a stepper motor system (New Focus), which allows the stage to be moved in 30 nm increments over a range of several mm.

D. Control software

The AFM is controlled entirely via subroutines written in MATLAB, which interface directly and robustly with the data acquisition system. A graphical user interface is used to simultaneously acquire data and output the necessary actuator wave forms, allowing real-time plotting of force curves and images (see Sec. VI). The software is freely available for educational use.[8]

E. Cost considerations

There are inevitable cost-performance tradeoffs in a measurement system; we designed ours to maximize accessibility to the student and usability for a variety of student experiments. The total system cost is approximately $10 000, for which some of the major components are listed in Table I.

Options for further reducing the cost include using a less expensive personal computer, replacing the rack instruments with custom dedicated electronics, and using a less expensive stage (at the expense of a reduction in stability, and therefore resolution).

V. THEORY

A. Noise PSD and transfer function

As suggested by Eq. (5), we would like to determine a function to describe the power spectral density (PSD) of the cantilever's position fluctuations, when driven by background thermal energy. By Parseval's relation, we know that integrating the positional PSD $S_{zz}(\omega)$ [units: m^2/Hz] gives the variance of the cantilever's positional coordinate z.

$$\langle z^2 \rangle = \int_0^\infty S_{zz}(\omega) d\omega. \tag{6}$$

We can rewrite $S_{zz}(\omega)$ as the product of a force PSD $S_{FF}(\omega)$ [N^2/Hz] and the square of an amplitude transfer function $G(\omega)$ [m/N]. The force spectrum S_{FF} is assumed to be white, and therefore has no frequency dependence and remains outside the integral. On the left-hand side, we substitute for the mean-square displacement from Eq. (3)

$$\frac{k_B T}{k} = S_{FF} \int_0^\infty G^2(\omega) d\omega. \tag{7}$$

To find the transfer function of the system $G(\omega)$ we begin with the force balance equation describing a damped harmonic oscillator with effective mass m and spring constant k, driven by an arbitrary force $F_0 \cos(\omega t)$

$$ma = F_0 \cos(\omega t) - kz - \frac{\omega_0 m}{Q} v. \tag{8}$$

The system is characterized by the resonant frequency $\omega_0 = \sqrt{k/m}$ and quality factor Q, which describes the degree of damping.[11] We rewrite Eq. (8) as a differential equation in z

$$\frac{d^2 z}{dt^2} + \frac{\omega_0}{Q} \frac{dz}{dt} + \omega_0^2 z = \frac{F_0}{m} \cos(\omega t). \tag{9}$$

We are interested only in the steady state solution of Eq. (9), which is completely described by the particular solution (the homogeneous solution only contributes a short transient at the start). The particular solution has the form

$$z(t) = A(\omega) \cos(\omega t + \phi), \tag{10}$$

where

$$A(\omega) = \frac{F_0/m}{\sqrt{(\omega_0^2 - \omega^2)^2 + \omega_0^2 \omega^2 / Q^2}}. \tag{11}$$

The amplitude $A(\omega)$ can also be represented as the product of the transfer function that we seek $G(\omega)$ and a force $A(\omega) = G(\omega) F_0$. We divide out the force, rearrange terms, and obtain

$$G(\omega) = \frac{1/k}{\sqrt{(1 - \omega^2/\omega_0^2)^2 + \omega^2/Q^2\omega_0^2}}. \tag{12}$$

We now substitute this transfer function into Eq. (7) to determine the value of S_{FF}. To do so, we evaluate

$$k_B T k = S_{FF} \int_0^\infty \frac{d\omega}{(1 - \omega^2/\omega_0^2)^2 + \omega^2/Q^2\omega_0^2}. \tag{13}$$

The solution for S_{FF} is

$$S_{FF} = \frac{4 k_B T k}{Q \omega_0}. \tag{14}$$

Finally, we are able to obtain the position PSD $S_{zz}(\omega)$ [m^2/Hz], which is used in Eq. (5) for curve fitting [note that Eq. (5) uses the square root form for correct units]

$$S_{zz}(\omega) = S_{FF}G^2(\omega) = \frac{4k_BT}{Qk\omega_0}\frac{1}{(1-\omega^2/\omega_0^2)^2 + \omega^2/Q^2\omega_0^2}. \tag{15}$$

We have found that students gain insight into the workings of the system if provided with a few equations such as Eqs. (3), (12), and (15), along with suitable explanations of what they represent. Understanding can be further enhanced by discussing this derivation prior to the laboratory session.

B. Calculating k_B

The results of Sec. V A suggest two calculations that can be used to find k_B. The more straightforward requires a measurement of the cantilever's positional variance $\langle z^2 \rangle$ in the time domain. The variance is substituted into Eq. (3), along with the cantilever's spring constant (see Sec. V C) to yield k_B. This procedure is problematic because the signal includes large amounts of $1/f$-type noise at low frequencies contributed by the electronics and environmental drifts. It is instructive to have the students determine the relative accuracy of this approach to the preferred method, which we describe next.

A somewhat more involved, but more accurate and elegant calculation is based on the fact that the displacement PSD [Eq. (15)] reduces to a simple expression in the low-frequency limit ($\omega \ll \omega_0$)

$$\delta_{LF}^2 = S_{zz}(\omega \ll \omega_0) = \frac{4k_BT}{Qk\omega_0}. \tag{16}$$

This expression represents the thermomechanical noise limit. In a real PSD it is obscured by $1/f$-type noise, which dominates at low frequencies. At frequencies around the cantilever's resonance peak, the true thermomechanical noise dominates, and fitting Eq. (5) to the measured spectrum near the peak allows a good estimate of δ_{LF} $[\mathrm{m}/\sqrt{\mathrm{Hz}}]$. This value is extracted from the fitted transfer function, along with the parameters ω_0 and Q, and they are used to calculate k_B from Eq. (16). The other parameter that is needed is the spring constant k.

C. Calculating the spring constant

AFM cantilever spring constants are most accurately determined by attaching a small known mass to their end and measuring the shift in their resonant frequency.[12] We prefer to use simpler analytical calculations, because they are sufficiently accurate for our purposes. Also, although we have not used this approach, the cantilever stiffness can be directly measured by bending it against a substrate of known stiffness with a well-calibrated position readout.[13]

Analytically, two calculations are available. The simplest comes from a basic mechanical beam-bending analysis of a rectangular cantilever (found in any introductory text on solid mechanics), for which the spring constant k can be expressed as

$$k = \frac{Ebh^3}{4L^3}, \tag{17}$$

where E is the elastic (Young's) modulus of the beam material, and L, b, and h are the length, width, and thickness of the beam, respectively. This method does not have high accuracy, due to its third-power dependence on L and h (the latter being prone to variations up to 10%).

Table II. Typical results of k_B calculations and the associated parameters.

Parameter (units)	350 μm device	275 μm device
k (N/m)	0.041	0.085
Q	20	30
ω_0 (kHz)	9.25	15.2
δ_{LF} (pm/$\sqrt{\mathrm{Hz}}$)	0.63	0.15
k_B (J/K)	1.6×10^{-23}	0.47×10^{-23}

A model that is less sensitive to geometrical inaccuracies has generally yielded slightly more accurate k values with our cantilevers. This model is based on the work of Sader and coworkers[14] and uses the cantilever's resonant frequency (obtained experimentally with high accuracy)

$$k = 0.2427\rho_c hbL\omega_{\mathrm{vac}}^2, \tag{18}$$

where ρ_c is the mass density of the material and ω_{vac} is the cantilever's resonant frequency in vacuum. To account for damping effects in air, we can reasonably assume that the resonant frequency in air $\omega_{\mathrm{air}} = \omega_0$ is 2% lower than ω_{vac} for the purposes of these calculations.

By the methods we have described, students can readily obtain k_B values accurate to within 50%. The main source of error is estimating the position of the laser spot on the ID grating, in order to calculate F_{corr} for calibration. Both methods of finding the spring constant depend on cantilever material properties (E and ρ_c), which are sometimes difficult to know accurately for thin films. These values can therefore become the major source of uncertainty and limit the accuracy of the measurement of k_B. Table II shows typical measured and calculated parameter values for various quantities involved in the measurements.

VI. OTHER POSSIBLE EXPERIMENTS

This AFM enables a number of other experiments. Imaging is probably most intuitively accessible to students and can readily be accomplished with the ID cantilever as described in Ref. 3. Figure 6(a) shows a scanning electron mi-

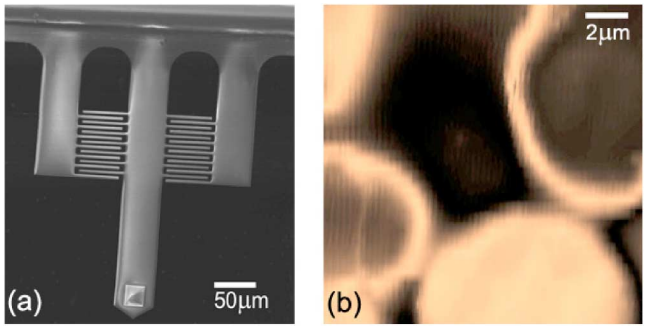

Fig. 6. (a) A scanning electron micrograph image of a cantilever probe used for imaging. This view is of the underside of the device, showing the integrated tip. The short side levers are used as fixed reference beams and do not contact the sample. (b) A sample image taken with the AFM of human red blood cells, imaged in air after they were dried on a glass substrate. The image is 15 μm square, and consists of 32 lines of data with 250 data points acquired per line. The image was linearly interpolated and up sampled to 400×400 pixels.

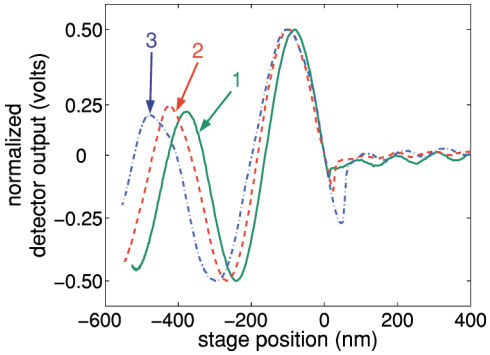

Fig. 7. Normalized data collected for an experiment to measure the elastic modulus. Force curve 1 was taken using a hard sample (silicon nitride), and curves 2 and 3 were taken using a compliant polymer (PDMS) of variable hardness. Each curve is an average of three data sets. For clarity, only the part of the curve corresponding to upward stage movement is shown (data points captured during downward stage motion are omitted). PDMS samples were prepared by mixing Dow Corning Sylgard 184 in ratios of 10:1 (2) and 25:1 (3), depositing a 1–2 mm layer onto a silicon substrate, then curing at 80 °C for 30 min. Modulus data can be extracted from analyzing the period of the detector output curve.

crograph of an ID cantilever designed for imaging; a constant-height mode image of red blood cells is shown in Fig. 6(b). Although the ID sensor can resolve displacements well below 1 Å, the height resolution of our system is on the order of a few nanometers in a 1 kHz bandwidth due to the large mechanical path between the cantilever and sample. The resolution could be improved by replacing the relatively large off-the-shelf mounting components with a custom-designed mount.

It is also possible to determine elastic moduli of structures or materials by using techniques based on measuring force-versus-distance curves.[15,16] Because the ID sensor is nonlinear, relative changes in local modulus can be measured by observing the shift in the periodicity of the sinusoidal force curve. To demonstrate this technique in our teaching lab, we used PDMS elastomer samples of various moduli. The resulting force-versus-distance curves are shown in Fig. 7.

Because our AFM was designed to incorporate the Veeco fluid cell[17] as the cantilever holder, it should be straightforward to image and conduct modulus measurements in an aqueous environment, thereby allowing students to develop assays for studying tissues, live cells, and ultimately single molecules.

ACKNOWLEDGMENTS

This work was supported by the Cambridge-MIT Institute and the Whitaker Foundation. Devices were fabricated at the MIT Microsystems Technology Laboratories.

[a]Electronic address: scottm@media.mit.edu

[1] R. S. Newrock, "A new course: The physical principles of biological instrumentation," Am. J. Phys. **46**(1), 32–34 (1978).

[2] G. Binnig, C. F. Quate, and Ch. Gerber, "Atomic Force Microscope," Phys. Rev. Lett. **56**(9), 930–933 (1986).

[3] S. R. Manalis, S. C. Minne, A. Atalar, and C. F. Quate, "Interdigital cantilevers for atomic force microscopy," Appl. Phys. Lett. **69**(25), 3944–3946 (1996).

[4] S. Alexander, L. Hellemans, O. Marti, J. Schneir, V. Elings, P. K. Hansma, M. Longmire, and J. Gurley, "An atomic-resolution atomic-force microscope implemented using an optical lever," J. Appl. Phys. **65**(1), 164–167 (1989).

[5] G. G. Yaralioglu, A. Atalar, S. R. Manalis, and C. F. Quate, "Analysis and design of an interdigital cantilever as a displacement sensor," J. Appl. Phys. **83**(12), 7405–7415 (1998).

[6] Stephen C. Minne, Scott R. Manalis, and Calvin F. Quate, *Bringing Scanning Probe Microscopy Up to Speed* (Kluwer, Norwell, MA, 1999), Chap. 4.

[7] F_{corr} can be estimated by assuming a quadratic shape for the bent cantilever $F_{corr}=1/m_{ID}^2$, where $m_{ID}=L_{ID}/L_T$ is the ratio of the distance of the ID fingers from the cantilever base to the total cantilever length. A more precise expression is $F_{corr}=2/(3m_{ID}^2-m_{ID}^3)$, which is derived from the equation for the shape of a simple rectangular beam, with an applied end-load P: $z(x)=Px^2(3L_T-x)/(6EI)$, where x is the coordinate along the length of the cantilever, and E and I are the elastic modulus and moment of inertia of the beam, respectively. The tip deflection in this case is therefore $z(L_T)=PL_T^3/(3EI)$.

[8] See ⟨http://web.mit.edu/be/teachAFM/⟩

[9] T. R. Albrecht, S. Akamine, T. E. Carver, and C. F. Quate, "Microfabrication of cantilever styli for the atomic force microscope," J. Vac. Sci. Technol. A **8**(4), 3386–3396 (1990).

[10] ⟨http://www.nnin.org/nnin_site.html⟩

[11] For simplicity, we omit the intermediate parameter γ that is typically used. For an introductory treatment of harmonic oscillators, see Atam P. Arya, *Introduction to Classical Mechanics* (Prentice Hall, Englewood Cliffs, 1998), 2nd ed., Chap. 3 or Richard P. Feynman, Robert B. Leighton, and Matthew L. Sands, *The Feynman Lectures on Physics* (Addison-Wesley, Reading, MA, 1989), Vol. 1, Chap. 23.

[12] J. P. Cleveland, S. Manne, D. Bocek, and P. K. Hansma, "A nondestructive method for determining the spring constant of cantilevers for scanning force microscopy," Rev. Sci. Instrum. **64**(2), 403–405 (1993).

[13] A. Torii, M. Sasaki, K. Hane, and S. Okuma, "A method for determining the spring constant of cantilevers for atomic force microscopy," Meas. Sci. Technol. **7**(2), 179–184 (1996).

[14] J. E. Sader, J. W. M. Chon, and P. Mulvaney, "Calibration of rectangular atomic force microscope cantilevers," Rev. Sci. Instrum. **70**(10), 3967–3969 (1999).

[15] A. L. Weisenhorn, M. Khorsandi, S. Kasas, V. Gotzos, and H.-J. Butt, "Deformation and height anomaly of soft surfaces studied with an AFM," Nanotechnology **4**(2), 106–113 (1993).

[16] A. Touhami, B. Nysten, and Y. F. Dufrêne, "Nanoscale mapping of the elasticity of microbial cells by atomic force microscopy," Langmuir **19**(11), 4539–4543 (2003).

[17] Veeco Contact Mode fluid cell, part # FC at ⟨http://www.veecoprobes.com⟩